Discovery of tandem and interspersed segmental duplications using high throughput sequencing

Arda Soylev [1 ‡], Thong Le [2,3 ‡], Hajar Amini [4], Can Alkan [1,5,6*] and Fereydoun Hormozdiari [2,7,8*]

[1] Department of Computer Engineering, Bilkent University, Ankara, 06800, Turkey

[2] UC-Davis Genome Center, University of California, Davis, CA, USA.

[3] Department of Computer Science, University of California, Davis, CA, USA.

[4] Department of Plant Biology, University of California, Davis, CA, USA.

[5] Bilkent-Hacettepe Health Sciences and Technologies Program, Ankara, 06800, Turkey

[6] Department of Computer Science, ETH Zürich, 8006, Switzerland

[7] Department of Biochemistry and Molecular Medicine, University of California, Davis, CA, USA.

[8] MIND Institute, University of California, Davis, CA, USA.

Abstract

Motivation: Several algorithms have been developed that use high throughput sequencing technology to characterize structural variations. Most of the existing approaches focus on detecting relatively simple types of SVs such as insertions, deletions, and short inversions. In fact, complex SVs are of crucial importance and several have been associated with genomic disorders. To better understand the contribution of complex SVs to human disease, we need new algorithms to accurately discover and genotype such variants. Additionally, due to similar sequencing signatures, inverted duplications or gene conversion events that include inverted segmental duplications are often characterized as simple inversions; and duplications and gene conversions in direct orientation may be called as simple deletions. Therefore, there is still a need for accurate algorithms to fully characterize complex SVs and thus improve calling accuracy of more simple variants.

Results: We developed novel algorithms to accurately characterize tandem, direct and inverted interspersed segmental duplications using short read whole genome sequencing data sets. We integrated these methods to our TARDIS tool, which is now capable of detecting various types of SVs using multiple sequence signatures such as read pair, read depth and split read. We evaluated the prediction performance of our algorithms through several experiments using both simulated and real data sets. In the simulation experiments, TARDIS achieved 97.67% sensitivity with only 1.12% false discovery rate. For experiments that involve real data, we used two haploid genomes (CHM1 and CHM13) and one human genome (NA12878) from the Illumina Platinum Genomes set. Comparison of our results with orthogonal PacBio call sets from the same genomes revealed higher accuracy for TARDIS than state of the art methods. Furthermore, we showed a surprisingly low false discovery rate of our approach for discovery of tandem, direct and inverted interspersed segmental duplications prediction on CHM1 (less than 5% for the top 50 predictions). The algorithms we describe here are the first to predict insertion location and the various types of new segmental duplications using HTS data.

Availability: TARDIS software is available at https://github.com/BilkentCompGen/tardis

Contact: fhormozd@ucdavis.edu and calkan@cs.bilkent.edu.tr

‡ These authors contributed equally. * Joint corresponding authors.

1 Introduction

Genomic differences between individuals of the same species, or among different species, range from single nucleotide variation (SNVs) [18] to small insertion/deletions (indels) [22] up to 50 bp, structural variation (SVs) [2] that affect >50 bp, and larger chromosomal aberrations [23]. Among these types of variants, SNVs were extensively and systematically studied since the introduction of microarrays, which can also be used to genotype short indels [18]. SVs, especially copy number variations (CNVs), were first identified using BAC arrays [27, 25], and then oligonucleotide array comparative genomic hybridization [28, 7] and SNV microarrays by analyzing allele frequencies[19, 8]. Chromosomal aberrations such as trisomy, or large translocations (e.g., Philadelphia chromosome [26]) can be tested using fluorescent in-situ hybridization [23].

Fine scale SV discovery was made possible using fosmid-end sequencing [36], and later indels were identified at breakpoint level using whole genome shotgun (WGS) sequencing data [22]. However, both approaches used the Sanger sequencing technology, which is prohibitively expensive to scale to analyze thousands of genomes. High throughput sequencing arose as a cost effective alternative [29] to characterize SVs first using the Roche/454 platform [14], and then Illumina [3, 9, 37, 21, 16, 30, 1, 37].

The 1000 Genomes Project, launched in 2008, used the HTS platforms to catalog SNVs, indels, and SVs in the genomes of 2,504 human individuals [35]. Many algorithms were developed that use one of four basic sequence signatures to discover SVs, namely read depth, read pair, split reads, and assembly [20, 2], however, most of these tools focus on characterizing only a few types of SVs. More modern SV callers such as DELLY [24], LUMPY [15], and TARDIS [31] integrate multiple sequencing signatures to identify a broader range of SVs such as deletions, novel insertions, inversions, and mobile element insertions. However, there is still a lack of accurate algorithms to characterize several forms of complex SVs, such as tandem or interspersed segmental duplications (SDs) [6, 5]. Note that read depth based methods can identify the *existence* of SDs [3, 33], but cannot detect the location of the new copies of the duplications.

Here we describe novel algorithms to accurately characterize both tandem and interspersed SDs using short read HTS data. Our algorithms make use of multiple sequence signatures to find approximate locations for the duplication insertion breakpoints. We integrated our methods into the TARDIS tool [31] therefore extending its capability to simultaneously detect various types of SVs. We test the new version of TARDIS using both simulated and real data sets. We show that TARDIS achieves 97.67% sensitivity with only 1.12% false discovery rate (FDR) in simulation experiments. We also used real WGS data sets generated from two haploid genomes (i.e., CHM1 [12] and CHM13 [32]). Comparison of our predictions with *de novo* assemblies generated using long reads from the same DNA resources [32] revealed ¡5% false discovery rate for the duplications with high score.

The algorithms we describe in this manuscript are the *first* methods to discover the insertion locations of segmental duplications using high throughput sequencing data. Coupled with the previously documented capability of TARDIS to identify deletions, novel and mobile element insertions, and inversions, we are one more step closer towards a comprehensive characterization of SVs in high throughput sequenced genomes.

2 Methods

2.1 Motivation

The 1000 Genomes Project provides a catalog of SVs in the genomes of 2,504 individuals from many populations [34]. The project primarily focused on characterizing deletions, insertions, and mobile element transpositions, however, it also generated a set of inversion calls. A careful analysis shows that a substantial fraction of the predicted inversions are in fact complex rearrangements that include duplications, inverted

duplications, and deletions within an inverted segment (Figure 1). This is because the read pair signatures that signal such complex SVs are exactly the same as shown in Fig. 2. Therefore, any algorithm based on read pair (and/or split read) signature may incorrectly classify these complex events as simple inversions, unless it tries to characterize all such events simultaneously, with additional probabilistic models to differentiate events that show themselves with the same signature.

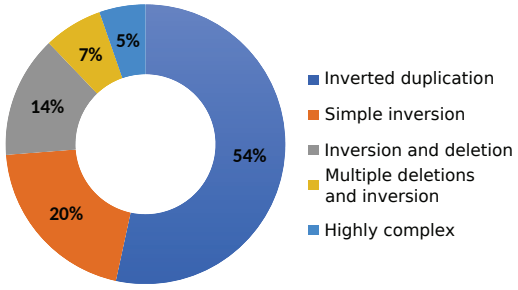

Figure 1: Relative abundance of complex SVs among the inversion calls reported in the 1000 Genomes Project [34]. 54% of predicted inversions are in fact inverted duplications and only 20% are correctly predicted as simple inversions.

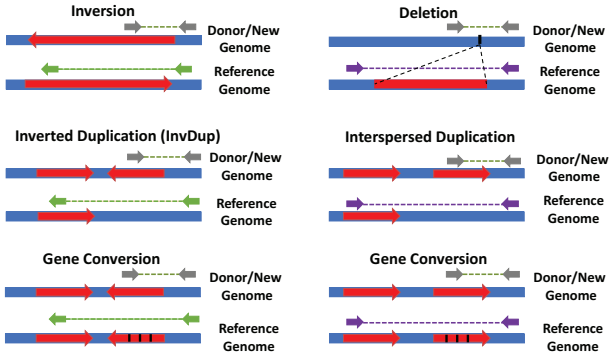

Figure 2: Read pair sequence signatures of inversions, deletions, inverted duplications, and gene conversions. Note that the signatures for inversions, inverted duplications, and inverted gene conversion events are exactly the same. Similarly, deletions, direct duplications and gene conversions with direct duplication show the same signature.

2.2 Read pair and split read clustering

TARDIS uses a combination of read pair, read depth and split read sequencing signatures to discover SVs [31]. TARDIS formulation is based on algorithms we developed earlier using maximum parsimony [9, 11] objective function. The proposed approach has two main steps: First clustering read pairs and split reads that signal each specific type of SV, and second apply a strategy to select a subset of clusters as predicted SV. In this paper we extend TARDIS to characterize a complex set of SVs, which are incorrectly categorized by state of the art methods for SV discovery. Specifically the methods we present here will **advance our**

capability in discovery of duplication based SVs. Furthermore, our new methods are capable of separating inversions from more complex events of inverted duplications and are also able to predict the insertion locations of the new copies of segmental duplications. We would argue that considering these more complex types of SV is crucial in improving the accuracy of predicting other types of SVs. Furthermore, we have modified TARDIS to calculate a likelihood score for each SV provided the observed read pair, read depth and split read signatures. Figure 3 summarizes the read pair signatures that TARDIS uses to find tandem and interspersed duplications in both direct and inverted orientation. Although not shown on the figure for simplicity, similar rules are required for split reads that signal the same types of SVs (Supplementary Figure 1).

2.2.1 Maximal valid clusters

We have previously described algorithms to calculate maximal valid clusters for deletions, inversions, and mobile element insertions [9, 10, 11, 31].

In this section we provide new methods to find maximum valid clusters for tandem and interspersed (both direct and inverted) duplications.

A valid cluster is a set of alignments of discordant read pairs and/or split reads that signal the same particular SV event denoted by

$$VClus_i = \{vc_1, vc_2, ..., vc_n\}$$

There are a set of rules that each vc_i should satisfy in order to support the cluster, $VClus_i$, based on the type of SV.

Inverted duplications : We assume the fragment sizes for read pairs are in the range $[\delta_{min}, \delta_{max}]$, and we denote the insertion breakpoint of the duplication as P_{Br} and the locus of the duplicated sequence is $[P_L, P_R]$ (Figure 3A). We scan the genome from beginning to end, and we consider each position as a potential duplication insertion breakpoint P_{Br}. We consider all sets of read pairs where both mates map to the same strand (i.e., $+/+$ and $-/-$) within interval $[P_{Br} - \delta_{max}, P_{Br}]$ and $[P_{Br}, P_{Br} + \delta_{max}]$ respectively as clusters that potentially signal an inverted duplication.

Interspersed direct duplications : We create the valid clusters in a way similar to the inverted duplications, with the exception of the required read mapping properties. For direct duplications we require each mate of a read pair to map to opposing strands (i.e., $+/-$ and $-/+$).

Tandem duplications : We also create the clusters for tandem duplications as shown in Figure 3. In the case of tandem duplications, discordant read pairs and split reads map in opposing strands, where the read mapping to the upstream location will map to the reverse strand, and the read mapping to downstream will map to the forward strand (i.e., $-/+$).

Similar to the valid cluster formulation, a maximal valid cluster is a valid cluster that encompasses all the valid read pairs and split reads for the particular SV event (i.e., no valid superset exists). This can be computed in polynomial time as follows:

1. We initially create maximal sets $S = \{S_1, S_2, ..., S_k\}$ that harbors the read pair/split read alignments $S_i = \{rp_1, rp_2, ..., rp_k\}$.

A

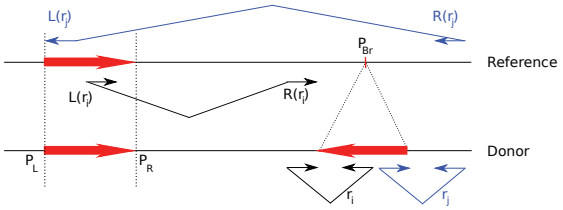

$$\delta_{min} < P_{Br} - R(r_i) + P_R - L(r_i) < \delta_{max}$$

$$\delta_{min} < R(r_j) - P_{Br} + L(r_j) - P_L < \delta_{max}$$

B

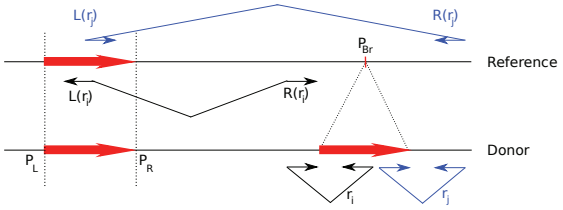

$$\delta_{min} < P_{Br} - R(r_i) + L(r_i) - L(r_i) < \delta_{max}$$

$$\delta_{min} < R(r_j) - P_{Br} + P_R - L(r_j) < \delta_{max}$$

C

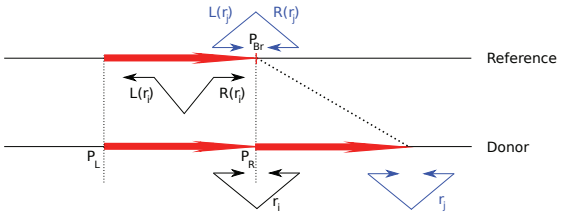

$$\delta_{min} < L(r_i) - P_L + P_R - R(r_i) < \delta_{max}$$

Figure 3: Read pair sequence signatures used in TARDIS to characterize A) interspersed duplications in inverted orientation, B) interspersed duplications in direct orientation, and C) tandem duplications.

2. For interspersed duplications, we use an additional step to bring mappings in both forward-forward and reverse-reverse (forward-reverse and reverse-forward for inverted duplications) orientations together inside the same set.

3. For each maximal overlapping set S_i found in step 1, we create all the overlapping maximal subsets s_i. (This step is necessary only for detecting inversions and interspersed duplications)

4. Among all the sets s_i found in Step 3, remove any set that is a proper subset of another chosen set.

2.3 Probabilistic Model

As we describe above different types of SVs may generate similar discordant read pair signatures (Figure 2). We therefore developed a probabilistic model that makes use of the read depth signature to assign a likelihood score to each potential SV. Our new probabilistic model has the ability to distinguish different types of SVs with the same read pair signature.

2.3.1 Likelihood model

Assume the set of maximum valid clusters $SV = \{S_1, S_2, \ldots, S_n\}$ is observed in the sequenced sample. TARDIS keeps track the following information for each maximum valid cluster S_i for $1 \leq i \leq n$:

- observed read depth and read pair information (d_i, p_i), i.e. d_i is the total observed read depth, and p_i is the number of discordantly mapped read pairs.
- potential duplicated or deleted or inverted region (α_i, β_i).
- potential breakpoint γ_i.
- potential SV type.

Assuming observed read depth and number of discordant read pairs follow a Poisson distribution, $\lambda > 0$,

$$\text{Poisson}(\lambda, x) = \frac{\lambda^x e^{-\lambda}}{x!}$$

here, λ is the expected number of read depth or read pairs, and x is the observed number of read depth or read pairs respectively. However, the expected read depth or read pairs for some events might be zero, we approximate the probability by,

$$\text{Poisson}(0, x) = \varepsilon^x$$

for a small $\varepsilon > 0$ (e.g. $\varepsilon = 0.01$ for read pairs and $\varepsilon = 0.001$ for read depth).

For each cluster S_i, we define a random variable $state_i \in \{0, 1, 2\}$ in which the state of S_i is *homozygous* if $state_i = 2$, *heterozygous* if $state_i = 1$, and *no event* if $state_i = 0$. We also define a random variable $type_i$, which represents the SV type for S_i. Given $state_i = k$ and $type_i = \delta$, the likelihood of S_i can be calculated as:

$$\begin{aligned} L_i(\delta, k) &= P(S_i \mid \delta, k) \\ &= P(\textit{ read depth of } S_i \mid \delta, k) \cdot P(\textit{ read pairs of } S_i \mid \delta, k) \\ &= \text{Poisson}(d_i, \lambda_d) \cdot \text{Poisson}(p_i, \lambda_p) \\ &= \frac{\lambda_d^{d_i} e^{-\lambda_d}}{d_i!} \cdot \frac{\lambda_p^{p_i} e^{-\lambda_p}}{p_i!} \end{aligned}$$

where λ_d is the expected read depth of S_i given $type_i = \delta, state_i = k$ and λ_p is the expected read pairs of S_i given $type_i = \delta, state_i = k$.

We calculate λ_d based on $(type_i, state_i)$ and the expected read depth within the region (α_i, β_i) normalized with respect to its G+C content using a sliding window of size 100 bp, denoted by $E_d[(\alpha_i, \beta_i)]$. We calculate λ_p based on the $(type_i, state_i)$ and the expected number of discordantly mapped read pairs around the potential breakpoint γ_i, denoted by $E_p[\gamma_i]$. For instance, if an event is categorized as homozygous deletion, we expect to see almost no read depth inside the potential deleted region (α_i, β_i), and the expected number of discordantly mapped read pairs should be approximately the expected number of reads containing the potential breakpoint, i.e $E_p[\gamma_j]$. For heterozygous deletion events, we expect to see half of the number of read depths and half of the expected number of discordantly mapped read pairs. We also calculate the likelihood score of no event at the potential region given that is categorized as deletion. For this case, we expect to

see the expected number of read depths in that potential region and zero discordantly mapped read pairs. Similarly, the value for λ_d, λ_p can be approximately for inversion and duplications. Table 1 shows the value for λ_d, λ_p for each $(type_i, state_i)$ using $E_d[(\alpha_i, \beta_i)]$ and $E_p[\gamma_i]$. Note that even though the formulation for λ_d, λ_p are the same for all types of duplications, the likelihood score will be different because the potential regions (α_i, β_i) are different based on the categorized type of the event being considered. Furthermore, the read-pair support and signature will be different for each type of duplication which is the key in resolving the type of duplication.

Table 1: Formulation for λ_d and λ_p for maximum valid cluster S_i

SV Type	State	λ_d	λ_p
Deletion	*homozygous*	0.0	$E_p[\gamma_i]$
	heterozygous	$0.5 \cdot E_d[(\alpha_i, \beta_i)]$	$0.5 \cdot E_p[\gamma_i]$
	no event	$E_d[(\alpha_i, \beta_i)]$	0.0
Inversion	*homozygous*	$E_d[(\alpha_i, \beta_i)]$	$E_p[\gamma_i]$
	heterozygous	$E_d[(\alpha_i, \beta_i)]$	$0.5 \cdot E_p[\gamma_i]$
	no event	$E_d[(\alpha_i, \beta_i)]$	0.0
Inverted Duplication	*homozygous*	$2 \cdot E_d[(\alpha_i, \beta_i)]$	$E_p[\gamma_i]$
	heterozygous	$1.5 \cdot E_d[(\alpha_i, \beta_i)]$	$0.5 \cdot E_p[\gamma_i]$
	no event	$E_d[(\alpha_i, \beta_i)]$	0.0
Direct Duplication	*homozygous*	$2 \cdot E_d[(\alpha_i, \beta_i)]$	$E_p[\gamma_i]$
	heterozygous	$1.5 \cdot E_d[(\alpha_i, \beta_i)]$	$0.5 \cdot E_p[\gamma_i]$
	no event	$E_d[(\alpha_i, \beta_i)]$	0.0
Tandem Duplication	*homozygous*	$2 \cdot E_d[(\alpha_i, \beta_i)]$	$E_p[\gamma_i]$
	heterozygous	$1.5 \cdot E_d[(\alpha_i, \beta_i)]$	$0.5 \cdot E_p[\gamma_i]$
	no event	$E_d[(\alpha_i, \beta_i)]$	0.0

2.3.2 SV weight

For each potential SV we calculate a score to represent how likely a SV prediction is correct given the observed signature. Note that, for each SV, we calculate the likelihood considering homozygous state and heterozygous state (i.e., 1/1 or 0/1 respectively) separately, and then select the larger value to approximate the likelihood of that prediction being correct. We define the score as log likelihood ratio of the putative SV being true given the observed data over it being false. Note that we use log function to avoid numerical errors. The score of potential SV S_i is defined as follows:

$$score(S_i) = \frac{\max\left(\log L_i(\delta_i, k=1), \log L_i(\delta_i, k=2)\right)}{\log L_i(\delta_i, k=0)}$$

where δ_i is the potential SV type of S_i. Again, $k = 0, 1, 2$ implies that the state of S_i is *no event*, *heterozygous*, *homozygous* respectively.

Then, the normalized weight of each cluster can be calculated as:

$$weight(S_i) = \frac{score(S_i)}{E_p[\gamma_i]}$$

2.3.3 Multi-mapping reads

We previously showed that a greedy approach motivated by weighted-set cover problem performs well in discovery of SVs with multiple mapping of the reads [9]. We therefore utilize a similar iterative approach

here: 1) at each step we select the set with the best SV weight, and 2) we assign the relative discordant read pairs and split reads to the selected SV and remove them from all other maximal clusters.

3 Results

3.1 Simulation

In order to evaluate performance of our SV detection algorithms, we developed a new simulator called CNVSim in Python to simulate five classes of SVs including deletions, inversions, tandem duplications, inverted duplications and interspersed direct duplications. We simulated SVs of lengths selected uniformly random between 500 bp and 10 Kbp. For inverted duplications and interspersed direct duplications, the distance from the new paralog to the original copy is chosen uniformly random between 5,000 bp and 50 Kbp. All segments are sampled randomly from the well-defined (i.e., no assembly gaps) regions in the reference genome, and guaranteed to be non-overlapping. Each simulated SV can be in homozygous or heterozygous state.

Based on the human reference genome (GRCh37), we simulated total of 1,200 SVs including 400 deletions, 200 inversions, 200 tandem duplications, 200 inverted duplications and 200 interspersed direct duplications. We then simulated WGS data at four depth of coverages 10X, 20X, 30X, 60X using wgsim (https://github.com/lh3/wgsim). We mapped the reads back to the human reference genome (GRCh37) using BWA-MEM [17]. Finally we obtained structural variation call sets using TARDIS, DELLY [24], and LUMPY [15].

Table 2: Summary of simulation predictions by TARDIS, LUMPY, and DELLY.

SV Type	Cov.	TARDIS		DELLY		LUMPY	
		FDR	TPR	FDR	TPR	FDR	TPR
Deletion	10X	**0.063**	0.933	0.312	**0.958**	0.315	0.790
	20X	**0.036**	0.950	0.329	**0.968**	0.327	0.943
	30X	**0.047**	0.960	0.330	**0.973**	0.328	0.948
	60X	**0.052**	0.965	0.330	**0.978**	0.329	0.958
Inversion	10X	0.025	0.970	0.482	**0.985**	**0.000**	0.945
	20X	0.011	0.980	0.495	**0.985**	**0.000**	0.965
	30X	0.003	**0.995**	0.495	0.960	**0.000**	0.970
	60X	0.009	**0.995**	0.495	0.990	**0.000**	0.970
Duplication	10X	**0.004**	**0.933**	0.204	0.500	0.202	0.408
	20X	**0.010**	**0.960**	0.202	0.515	0.205	0.498
	30X	**0.004**	**0.967**	0.204	0.515	0.202	0.502
	60X	**0.018**	**0.970**	0.205	0.518	0.206	0.502

We show the true positive rate/recall and false discovery rates (TPR and FDR) of TARDIS, LUMPY, and DELLY at different depths of coverage from 10X to 60X for deletions (Del), inversions (Inv), and segmental duplications (Dup). Note that LUMPY and DELLY can not predict interspersed segmental duplications, therefore these tools miss such events. TARDIS consistently shows low FDR with comparable sensitivity. In our simulation, the length of each SV is generated uniformly random between 500 bp and 10 Kbp.

Table 2 shows the true positive rate (TPR) and false discovery rate (FDR) of TARDIS compared to DELLY and LUMPY on the simulated data. The sensitivity of TARDIS is comparable to others for deletions and inversions, but TARDIS achieved a substantially higher TDR for tandem duplications. Additionally, TARDIS suffered very low FDR compared to the other tools we tested.

Furthermore, TARDIS can classify duplications into tandem, interspersed directed duplication and inverted duplication. However, DELLY and LUMPY are not designed to characterize interspersed segmental

Table 3: Characterization of different types of segmental duplications using TARDIS on simulated data.

Duplication Type	Coverage	Total Calls	Missed	TRUE	TPR	FALSE	FDR
Inverted Interspersed Duplication	10X	200	10	190	0.950	2	0.010
	20X	200	7	193	0.965	4	0.019
	30X	200	7	193	0.965	2	0.009
	60X	200	7	193	0.965	14	0.047
Direct Interspersed Duplication	10X	200	18	182	0.910	1	0.004
	20X	200	8	192	0.960	1	0.003
	30X	200	7	193	0.965	1	0.003
	60X	200	6	194	0.970	2	0.006
Tandem Duplication	10X	200	16	184	0.920	14	0.057
	20X	200	11	189	0.945	15	0.050
	30X	200	8	192	0.960	6	0.017
	60X	200	6	194	0.970	11	0.028

TARDIS can classify duplications into tandem, interspersed directed duplication and inverted duplication. However, DELLY and LUMPY are not designed to characterize these complex SVs. This table shows the true positive rate (recall) and false discovery rate (TPR and FDR respectively) of TARDIS for each type of duplication.

Table 4: 50 highest scoring segmental duplications predicted by TARDIS in the CHM1 genome.

Duplication Insertion Locus				TARDIS Dup. Type	TARDIS Score	Validation (PacBio)	Duplication Insertion Locus				TARDIS Dup. Type	TARDIS Score	Validation (PacBio)
chr11	63,698,518	-	63,702,043	Direct	0.000139	True	chr2	37,928,244	-	38,101,822	Tandem	0.000073	N/A
chr3	194,542,832	-	194,546,551	Direct	0.000147	True	chr20	60,032,847	-	60,033,402	Tandem	0.000118	True
chr5	143,512,368	-	143,515,435	Direct	0.000189	True	chr1	207,097,488	-	207,097,792	Tandem	0.000143	True
chr4	190,606,509	-	190,610,728	Direct	0.000356	True (Tandem)	chr5	3,323,854	-	3,324,308	Tandem	0.000150	N/A
chr20	2,359,601	-	2,360,962	Direct	0.000418	True	chr7	2,554,438	-	2,554,794	Tandem	0.000157	True
chr9	112,285,745	-	112,286,960	Direct	0.000422	True	chr12	110,099,331	-	110,099,745	Tandem	0.000164	True
chr19	4,511,103	-	4,511,949	Direct	0.000453	True (Tandem)	chr6	168,052,169	-	168,052,467	Tandem	0.000164	True
chr17	46,615,511	-	46,617,628	Direct	0.000466	True	chr16	86,008,690	-	86,009,146	Tandem	0.000174	True
chr18	69,711,699	-	69,713,216	Direct	0.000469	True	chr10	127,513,387	-	127,513,671	Tandem	0.000181	True
chr6	160,877,581	-	160,956,646	Direct	0.000484	N/A	chr14	106,049,119	-	106,049,358	Tandem	0.000181	True
chr2	10,825,652	-	10,827,218	Inverted	0.000118	True	chr17	80,317,606	-	80,318,018	Tandem	0.000181	N/A
chr3	43,834,994	-	43,836,299	Inverted	0.000123	True	chr20	62,720,019	-	62,720,214	Tandem	0.000181	True
chr2	125,051,481	-	125,053,239	Inverted	0.000127	True	chr9	132,158,786	-	132,159,087	Tandem	0.000181	N/A
chr14	67,169,917	-	67,171,999	Inverted	0.000146	True	chr10	132,974,718	-	132,975,317	Tandem	0.000190	True
chr2	72,440,066	-	72,441,647	Inverted	0.000159	True	chr12	13,164,410	-	13,164,785	Tandem	0.000190	True
chr10	127,190,469	-	127,197,324	Inverted	0.000190	True	chr8	2,215,816	-	2,216,235	Tandem	0.000201	N/A
chr9	107,816,536	-	107,817,623	Inverted	0.000200	True	chr6	44,012,337	-	44,012,939	Tandem	0.000211	True
chr17	36,350,020	-	36,407,396	Inverted	0.000208	False	chr9	34,681,543	-	34,681,898	Tandem	0.000266	True
chr12	71,532,693	-	71,534,000	Inverted	0.000318	True	chr6	35,754,611	-	35,766,730	Tandem	0.000273	True
chr1	114,645,854	-	114,654,623	Inverted	0.000334	True	chr20	59,567,846	-	59,590,250	Tandem	0.000287	True
chr18	11,508,829	-	11,511,479	Inverted	0.000353	True	chr20	62,123,611	-	62,124,191	Tandem	0.000355	True
chr5	115,346,294	-	115,351,084	Inverted	0.000390	True	chr18	77,831,328	-	77,831,783	Tandem	0.000369	N/A
chr7	31,586,823	-	31,590,394	Inverted	0.000437	True	chrX	417,957	-	418,352	Tandem	0.000369	True
chr19	15,785,635	-	15,888,539	Inverted	0.000485	True (Tandem)	chr20	42,325,185	-	42,325,572	Tandem	0.000399	True
							chr10	127,940,156	-	127,940,689	Tandem	0.000452	True
							chr3	197,117,149	-	197,117,806	Tandem	0.000463	N/A

Here we list the insertion locations of the top 50 scoring segmental duplications in CHM1 genome. All predictions are sorted by the SV score (lower is better). If the validation is N/A, that means the incorrect prediction from PacBio data, which will be skipped in the comparison. TARDIS only gives one false call and three interspersed duplications that are wrongly assigned to tandem duplications.

duplications, therefore we cannot provide comparisons. Table 3 shows the TDR, FDR, and the exact count of the number of True/False predictions for each type of segmental duplication.

3.2 Haploid genome analyses

As the first experiment with real data sets, we downloaded short read HTS data generated from two haploid cell lines, namely CHM1 and CHM13 [13, 32]. We mapped the reads to human reference genome (GRCh37) using BWA-MEM [17]. We also obtained call sets generated with PacBio data from the same genomes [4], but here we use updated SV calls (Mark Chaisson, personal communication), which we use as the true inversion set to compare with our predictions.

We present the comparison of the inversion predictions made by TARDIS and two state of the art methods LUMPY and DELLY in Figure 4. Note that we only consider inversions of length > 100 bp. Figure 4) (a) & (b) show the comparison of TARDIS predictions with those of other tools on CHM1 and CHM13 respectively. Overall, TARDIS achieves better area under the curve (AUC) statistic. We also tested the highest scoring set (n=50) of predicted inversions by each tool generated for the CHM1 genome. Briefly, we used a reference-guided *de novo* assembly of PacBio reads generated from the same genome [4] and mapped the contigs to the loci of interest (Figure 4) (c)). We show a ROC-like plot that uses actual numbers of true and false calls instead of rates (TPR/FDR). Here we observe again that compared to LUMPY and DELLY, TARDIS achieves better AUC. However, we note that the main reason for DELLY and LUMPY curves being closer to that of TARDIS for low number of false calls is because there were several predictions for which corresponding contigs did not exist in the assembled genome, therefore omitted from this plot.

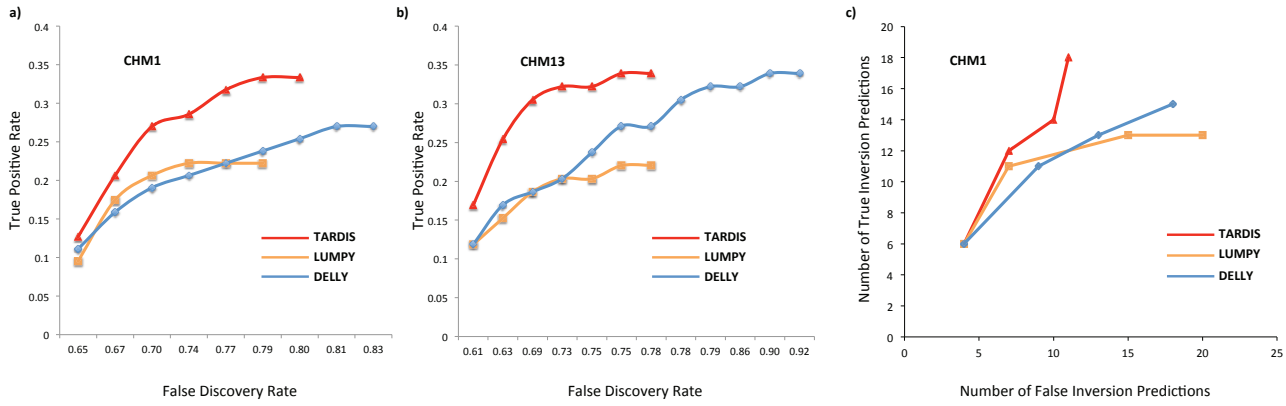

Figure 4: Receiver operator characteristic (ROC) curve of comparison of inversion predictions on CHM1 and CHM13. Overall TARDIS achieves better area under the curve (AUC) statistic that the two other approaches tested. (a), (b) comparison of CHM1 and CHM13 predicted inversions using PacBio reads based on BLASR mappings. (c) validation of top predicted inversion of different tools using local assembly of the PacBio reads of CHM1.

We provide the full set of the 50 highest scoring segmental duplications that TARDIS predicts in the CHM1 genome together with *in silico* validation using the corresponding PacBio-based assembly (Table 4). Almost all of the predicted duplications, except one, were validated using long reads. We provide the PacBio alignments of some of these events in the Supplementary Materials. Note that in most cases TARDIS assigned the correct subtype of duplications (inverted, direct or tandem duplication) to the prediction. As expected, the highest number of segmental duplications in the top 50 were tandem duplications ($> 50\%$ of all duplications).

3.3 NA12878 genome

We also analyzed the WGS data generated from NA12878 using TARDIS for various types of SV discovery and compared the results against state-of-the-art methods for inversion prediction. Similar to the simulation and CHM1/13 results, TARDIS outperformed the tested methods for SV discovery (see Supplementary Figure 2 for inversion comparison with a set of validated inversions on this sample).

More interestingly, we have found an example of a large inverted duplication in NA12878 sample which we validated using available orthogonal PacBio data generated from the same sample (Figure 5). The interesting point about this inverted duplication is that it is larger than 10 Kbp and the distance between locus of insertion and the duplicated region is also larger, which shows a potential start of a new segmental duplication.

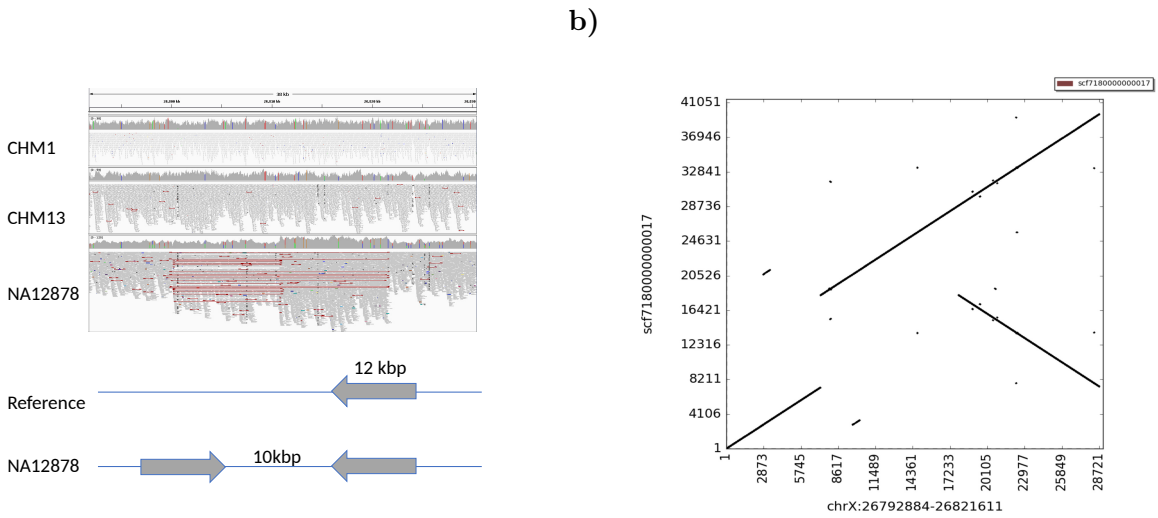

Figure 5: a) Illumina signature for an inverted duplication, b) PacBio validation.

4 Discussion

Characterization of structural variants using HTS data is a well-studied problem. Still, due to the difficulty of accurately predicting complex variants, most of the current approaches mainly focus on specific forms of SVs. In this paper we describe novel algorithms to detect complex SV events such as tandem, direct and inverted interspersed segmental duplications simultaneously with simpler forms SV using whole genome sequencing data. Our approach integrates multiple sequence signatures to identify and cluster potential SV regions under the assumption of maximum parsimony. However, complex SV events usually generate similar signatures (i.e., inversion vs. inverted duplication), which make it difficult to differentiate particular SV types. Therefore, we strengthened our method by using a probabilistic likelihood model to overcome this obstacle by calculating a likelihood score for each SV.

Using simulated and real data sets, we showed that TARDIS outperforms state-of-the art methods in terms of specificity for all types of SVs, and achieves considerably high true discovery rate for segmental duplications. It should be noted that it TARDIS is currently the only method that can classify duplications as tandem and interspersed in direct or inverted orientation using HTS data. Additionally, it demonstrates comparable sensitivity in deletions and inversions.

Future improvements in TARDIS will include addition of local assembly signature to help it achieve better accuracy. Although simulation experiments demonstrated potential efficacy of TARDIS in segmental duplication predictions, those that are generated from real genomes need to be experimentally verified to fully understand the power and shortcomings of the TARDIS algorithm. We can then apply TARDIS to thousands of genomes that were already sequenced as part of various projects, such as the 1000 Genomes Project to advance our understanding of the SV spectrum in human genomes. Another possible direction for TARDIS can be integration of new methods to better detect somatic structural variation detection, which we can then apply to cancer genomes.

Acknowledgements

We thank E. Ebren and F. Karaoglanoglu for their help in creating simulation data sets. We would thank Evan E. Eichler for insightful advise and comments. Part of the work was done during FH postdoc training in Evan E. Eichler's lab. We would also like to Mark Chaisson for providing PacBio call sets for CHM1 and CHM13, and also the local assembly of these genomes.

Funding

This work was supported by a grant by TÜBİTAK (215E172) and an EMBO Installation Grant (IG-2521) to C.A. The authors also acknowledge the Computational Genomics Summer Institute funded by NIH grant GM112625 that fostered international collaboration among the groups involved in this project.

Availability

TARDIS is available under BSD 3-clause license at `https://github.com/BilkentCompGen/tardis`, and the CNVSim simulator is available at `https://github.com/LeMinhThong/CNVSim`. NA12878 WGS data set can be downloaded from `https://www.illumina.com/platinumgenomes.html`. SRA IDs for CHM1 and CHM13 are SRP044331 and SRP080317, respectively. GenBank assembly accession numbers for CHM1 and CHM13 assemblies are GCA_000306695.2 and GCA_000983455.2.

References

[1] Alexej Abyzov, Alexander E. Urban, Michael Snyder, and Mark Gerstein. CNVnator: an approach to discover, genotype, and characterize typical and atypical CNVs from family and population genome sequencing. *Genome Res*, 21(6):974–984, Jun 2011.

[2] Can Alkan, Bradley P Coe, and Evan E Eichler. Genome structural variation discovery and genotyping. *Nat Rev Genet*, 12(5):363–376, May 2011.

[3] Can Alkan, Jeffrey M Kidd, Tomas Marques-Bonet, Gozde Aksay, Francesca Antonacci, Fereydoun Hormozdiari, Jacob O Kitzman, Carl Baker, Maika Malig, Onur Mutlu, S. Cenk Sahinalp, Richard A Gibbs, and Evan E Eichler. Personalized copy number and segmental duplication maps using next-generation sequencing. *Nat Genet*, 41(10):1061–1067, Oct 2009.

[4] Mark J P. Chaisson, John Huddleston, Megan Y. Dennis, Peter H. Sudmant, Maika Malig, Fereydoun Hormozdiari, Francesca Antonacci, Urvashi Surti, Richard Sandstrom, Matthew Boitano, Jane M. Landolin, John A. Stamatoyannopoulos, Michael W. Hunkapiller, Jonas Korlach, and Evan E. Eichler. Resolving the complexity of the human genome using single-molecule sequencing. *Nature*, 517:608–611, Jan 2015.

[5] Mark J.P. Chaisson, Ashley D. Sanders, Xuefang Zhao, Ankit Malhotra, David Porubsky, Tobias Rausch, Eugene J. Gardner, Oscar Rodriguez, Li Guo, Ryan L. Collins, Xian Fan, Jia Wen, Robert E. Handsaker, Susan Fairley, Zev N. Kronenberg, Xiangmeng Kong, Fereydoun Hormozdiari, Dillon Lee, Aaron M. Wenger, Alex Hastie, Danny Antaki, Peter Audano, Harrison Brand, Stuart Cantsilieris, Han Cao, Eliza Cerveira, Chong Chen, Xintong Chen, Chen-Shan Chin, Zechen Chong, Nelson T. Chuang, Deanna M. Church, Laura Clarke, Andrew Farrell, Joey Flores, Timur Galeev, Gorkin David, Madhusudan Gujral, Victor Guryev, William Haynes-Heaton, Jonas Korlach, Sushant Kumar, Jee Young Kwon, Jong Eun Lee, Joyce Lee, Wan-Ping Lee, Sau Peng Lee, Patrick Marks, Karine Valud-Martinez, Sascha Meiers, Katherine M. Munson, Fabio Navarro, Bradley J. Nelson, Conor Nodzak, Amina Noor, Sofia Kyriazopoulou-Panagiotopoulou, Andy Pang, Yunjiang Qiu, Gabriel Rosanio, Mallory Ryan, Adrian Stutz, Diana C.J. Spierings, Alistair Ward, AnneMarie E. Welsch, Ming Xiao, Wei Xu, Chengsheng Zhang, Qihui Zhu, Xiangqun Zheng-Bradley, Goo Jun, Li Ding, Chong Lek Koh, Bing Ren, Paul Flicek, Ken Chen, Mark B. Gerstein, Pui-Yan Kwok, Peter M. Lansdorp, Gabor Marth, Jonathan Sebat, Xinghua Shi, Ali Bashir, Kai Ye, Scott E. Devine, Michael Talkowski, Ryan E. Mills, Tobias Marschall, Jan Korbel, Evan E. Eichler, and Charles Lee. Multi-platform discovery of haplotype-resolved structural variation in human genomes. *bioRxiv*, 2017.

[6] M.J.P. Chaisson, R.K. Wilson, and E. E. Eichler. Genetic variation and the de novo assembly of human genomes. *Nature Reviews Genetics*, 16:627–640, November 2015.

[7] Donald F Conrad, Dalila Pinto, Richard Redon, Lars Feuk, Omer Gokcumen, Yujun Zhang, Jan Aerts, T. Daniel Andrews, Chris Barnes, Peter Campbell, Tomas Fitzgerald, Min Hu, Chun Hwa Ihm, Kati Kristiansson, Daniel G Macarthur, Jeffrey R Macdonald, Ifejinelo Onyiah, Andy Wing Chun Pang, Sam Robson, Kathy Stirrups, Armand Valsesia, Klaudia Walter, John Wei, Wellcome Trust Case Control Consortium, Chris Tyler-Smith, Nigel P Carter, Charles Lee, Stephen W Scherer, and Matthew E Hurles. Origins and functional impact of copy number variation in the human genome. *Nature*, 464(7289):704–712, Apr 2010.

[8] Gregory M Cooper, Troy Zerr, Jeffrey M Kidd, Evan E Eichler, and Deborah A Nickerson. Systematic assessment of copy number variant detection via genome-wide SNP genotyping. *Nat Genet*, 40(10):1199–1203, Oct 2008.

[9] Fereydoun Hormozdiari, Can Alkan, Evan E Eichler, and S. Cenk Sahinalp. Combinatorial algorithms for structural variation detection in high-throughput sequenced genomes. *Genome Res*, 19(7):1270–1278, Jul 2009.

[10] Fereydoun Hormozdiari, Can Alkan, Mario Ventura, Iman Hajirasouliha, Maika Malig, Faraz Hach, Deniz Yorukoglu, Phuong Dao, Marzieh Bakhshi, S. Cenk Sahinalp, and Evan E Eichler. Alu repeat discovery and characterization within human genomes. *Genome Res*, 21(6):840–849, Jun 2011.

[11] Fereydoun Hormozdiari, Iman Hajirasouliha, Andrew McPherson, Evan E Eichler, and S. Cenk Sahinalp. Simultaneous structural variation discovery among multiple paired-end sequenced genomes. *Genome Res*, 21(12):2203–2212, Dec 2011.

[12] John Huddleston, Mark Jp Chaisson, Karyn Meltz Steinberg, Wes Warren, Kendra Hoekzema, David S Gordon, Tina A Graves-Lindsay, Katherine M Munson, Zev N Kronenberg, Laura Vives, Paul Peluso, Matthew Boitano, Chen-Shin Chin, Jonas Korlach, Richard K Wilson, and Evan E Eichler. Discovery and genotyping of structural variation from long-read haploid genome sequence data. *Genome research*, November 2016.

[13] John Huddleston, Swati Ranade, Maika Malig, Francesca Antonacci, Mark Chaisson, Lawrence Hon, Peter H. Sudmant, Tina A. Graves, Can Alkan, Megan Y. Dennis, Richard K. Wilson, Stephen W. Turner, Jonas Korlach, and Evan E. Eichler. Reconstructing complex regions of genomes using long-read sequencing technology. *Genome Res*, 24(4):688–696, Apr 2014.

[14] Jan O Korbel, Alexander Eckehart Urban, Jason P Affourtit, Brian Godwin, Fabian Grubert, Jan Fredrik Simons, Philip M Kim, Dean Palejev, Nicholas J Carriero, Lei Du, Bruce E Taillon, Zhoutao Chen, Andrea Tanzer, A. C Eugenia Saunders, Jianxiang Chi, Fengtang Yang, Nigel P Carter, Matthew E Hurles, Sherman M Weissman, Timothy T Harkins, Mark B Gerstein, Michael Egholm, and Michael Snyder. Paired-end mapping reveals extensive structural variation in the human genome. *Science*, 318(5849):420–426, Oct 2007.

[15] Ryan M. Layer, Colby Chiang, Aaron R. Quinlan, and Ira M. Hall. LUMPY: a probabilistic framework for structural variant discovery. *Genome Biol*, 15(6):R84, 2014.

[16] Seunghak Lee, Fereydoun Hormozdiari, Can Alkan, and Michael Brudno. MoDIL: detecting small indels from clone-end sequencing with mixtures of distributions. *Nat Methods*, 6(7):473–474, Jul 2009.

[17] Heng Li. Aligning sequence reads, clone sequences and assembly contigs with BWA-MEM. *arXiv preprint arXiv:1303.3997*, 2013.

[18] G. T. Marth, I. Korf, M. D. Yandell, R. T. Yeh, Z. Gu, H. Zakeri, N. O. Stitziel, L. Hillier, P. Y. Kwok, and W. R. Gish. A general approach to single-nucleotide polymorphism discovery. *Nat Genet*, 23(4):452–456, Dec 1999.

[19] Steven A. McCarroll, Tracy N. Hadnott, George H. Perry, Pardis C. Sabeti, Michael C. Zody, Jeffrey C. Barrett, Stephanie Dallaire, Stacey B. Gabriel, Charles Lee, Mark J. Daly, David M. Altshuler, and International HapMap Consortium . Common deletion polymorphisms in the human genome. *Nat Genet*, 38(1):86–92, Jan 2006.

[20] Paul Medvedev and Michael Brudno. *Ab Initio Whole Genome Shotgun Assembly with Mated Short Reads*, pp. 50–64. Springer Berlin Heidelberg, Berlin, Heidelberg, 2008.

[21] Paul Medvedev, Monica Stanciu, and Michael Brudno. Computational methods for discovering structural variation with next-generation sequencing. *Nat Methods*, 6(11 Suppl):S13–S20, Nov 2009.

[22] Ryan E Mills, Christopher T Luttig, Christine E Larkins, Adam Beauchamp, Circe Tsui, W. Stephen Pittard, and Scott E Devine. An initial map of insertion and deletion (INDEL) variation in the human genome. *Genome Res*, 16(9):1182–1190, Sep 2006.

[23] G Obe, P Pfeiffer, J R K Savage, C Johannes, W Goedecke, P Jeppesen, A T Natarajan, W Martínez-López, G A Folle, and M E Drets. Chromosomal aberrations: formation, identification and distribution. *Mutation research*, 504:17–36, July 2002.

[24] Tobias Rausch, Thomas Zichner, Andreas Schlattl, Adrian M. Stütz, Vladimir Benes, and Jan O. Korbel. DELLY: structural variant discovery by integrated paired-end and split-read analysis. *Bioinformatics*, 28(18):i333–i339, Sep 2012.

[25] Richard Redon, Shumpei Ishikawa, Karen R Fitch, Lars Feuk, George H Perry, T. Daniel Andrews, Heike Fiegler, Michael H Shapero, Andrew R Carson, Wenwei Chen, Eun Kyung Cho, Stephanie Dallaire, Jennifer L Freeman, Juan R González, Mònica Gratacòs, Jing Huang, Dimitrios Kalaitzopoulos, Daisuke Komura, Jeffrey R MacDonald, Christian R Marshall, Rui Mei, Lyndal Montgomery, Kunihiro Nishimura, Kohji Okamura, Fan Shen, Martin J Somerville, Joelle Tchinda, Armand Valsesia, Cara Woodwark, Fengtang Yang, Junjun Zhang, Tatiana Zerjal, Jane Zhang, Lluis Armengol, Donald F Conrad, Xavier Estivill, Chris Tyler-Smith, Nigel P Carter, Hiroyuki Aburatani, Charles Lee, Keith W Jones, Stephen W Scherer, and Matthew E Hurles. Global variation in copy number in the human genome. *Nature*, 444(7118):444–454, Nov 2006.

[26] J D Rowley. Letter: A new consistent chromosomal abnormality in chronic myelogenous leukaemia identified by quinacrine fluorescence and giemsa staining. *Nature*, 243:290–293, June 1973.

[27] Jonathan Sebat, B. Lakshmi, Jennifer Troge, Joan Alexander, Janet Young, Pär Lundin, Susanne Månér, Hillary Massa, Megan Walker, Maoyen Chi, Nicholas Navin, Robert Lucito, John Healy, James Hicks, Kenny Ye, Andrew Reiner, T Conrad Gilliam, Barbara Trask, Nick Patterson, Anders Zetterberg, and Michael Wigler. Large-scale copy number polymorphism in the human genome. *Science*, 305(5683):525–528, Jul 2004.

[28] Andrew J Sharp, Sierra Hansen, Rebecca R Selzer, Ze Cheng, Regina Regan, Jane A Hurst, Helen Stewart, Sue M Price, Edward Blair, Raoul C Hennekam, Carrie A Fitzpatrick, Rick Segraves, Todd A Richmond, Cheryl Guiver, Donna G Albertson, Daniel Pinkel, Peggy S Eis, Stuart Schwartz, Samantha J L Knight, and Evan E Eichler. Discovery of previously unidentified genomic disorders from the duplication architecture of the human genome. *Nat Genet*, 38(9):1038–1042, Sep 2006.

[29] Jay Shendure and Hanlee Ji. Next-generation DNA sequencing. *Nat Biotechnol*, 26(10):1135–1145, Oct 2008.

[30] Suzanne Sindi, Elena Helman, Ali Bashir, and Benjamin J Raphael. A geometric approach for classification and comparison of structural variants. *Bioinformatics*, 25:i222–i230, June 2009.

[31] Arda Soylev, Can Kockan, Fereydoun Hormozdiari, and Can Alkan. Toolkit for automated and rapid discovery of structural variants. *Methods*, 129:3–7, 2017.

[32] Karyn Meltz Steinberg, Valerie A. Schneider, Tina A. Graves-Lindsay, Robert S. Fulton, Richa Agarwala, John Huddleston, Sergey A. Shiryev, Aleksandr Morgulis, Urvashi Surti, Wesley C. Warren, Deanna M. Church, Evan E. Eichler, and Richard K. Wilson. Single haplotype assembly of the human genome from a hydatidiform mole. *Genome Res*, 24(12):2066–2076, Dec 2014.

[33] Peter H Sudmant, Jacob O Kitzman, Francesca Antonacci, Can Alkan, Maika Malig, Anya Tsalenko, Nick Sampas, Laurakay Bruhn, Jay Shendure, 1000 Genomes Project, and Evan E Eichler. Diversity of human copy number variation and multicopy genes. *Science*, 330(6004):641–646, Oct 2010.

[34] Peter H. Sudmant, Swapan Mallick, Bradley J. Nelson, Fereydoun Hormozdiari, Niklas Krumm, John Huddleston, Bradley P. Coe, Carl Baker, Susanne Nordenfelt, Michael Bamshad, Lynn B. Jorde,

Olga L. Posukh, Hovhannes Sahakyan, W. Scott Watkins, Levon Yepiskoposyan, M. Syafiq Abdullah, Claudio M. Bravi, Cristian Capelli, Tor Hervig, Joseph T. S. Wee, Chris Tyler-Smith, George van Driem, Irene Gallego Romero, Aashish R. Jha, Sena Karachanak-Yankova, Draga Toncheva, David Comas, Brenna Henn, Toomas Kivisild, Andres Ruiz-Linares, Antti Sajantila, Ene Metspalu, Jüri Parik, Richard Villems, Elena B. Starikovskaya, George Ayodo, Cynthia M. Beall, Anna Di Rienzo, Michael F. Hammer, Rita Khusainova, Elza Khusnutdinova, William Klitz, Cheryl Winkler, Damian Labuda, Mait Metspalu, Sarah A. Tishkoff, Stanislav Dryomov, Rem Sukernik, Nick Patterson, David Reich, and Evan E. Eichler. Global diversity, population stratification, and selection of human copy-number variation. *Science*, 349(6253), 2015.

[35] The 1000 Genomes Project Consortium. A global reference for human genetic variation. *Nature*, 526(7571):68–74, Sep 2015.

[36] Eray Tuzun, Andrew J Sharp, Jeffrey A Bailey, Rajinder Kaul, V. Anne Morrison, Lisa M Pertz, Eric Haugen, Hillary Hayden, Donna Albertson, Daniel Pinkel, Maynard V Olson, and Evan E Eichler. Fine-scale structural variation of the human genome. *Nat Genet*, 37(7):727–732, Jul 2005.

[37] Kai Ye, Marcel H Schulz, Quan Long, Rolf Apweiler, and Zemin Ning. Pindel: a pattern growth approach to detect break points of large deletions and medium sized insertions from paired-end short reads. *Bioinformatics*, 25(21):2865–2871, Nov 2009.